Journal of Neuroscience Methods 195 (2011) 15–23

Contents lists available at ScienceDirect

Journal of Neuroscience Methods

journal homepage: www.elsevier.com/locate/jneumeth

The membrane chamber: A new type of *in vitro* recording chamber

M.R.H. Hill*, S.A. Greenfield

Dept. of Pharmacology, University of Oxford, Mansfield Road, OX1 3QT, Oxford, United Kingdom

ARTICLE INFO

Article history:
Received 17 August 2010
Received in revised form 11 October 2010
Accepted 24 October 2010

Keywords:
In vitro
Brain slice
Recording chamber
Optical imaging
Voltage sensitive dye imaging
Perfusion

ABSTRACT

In vitro brain slice electrophysiology is a powerful and highly successful technique where a thin slice is cut from the brain and kept alive artificially in a recording chamber. The design of this recording chamber is pivotal to the success and the quality of such experiments. Most often one of two types of chambers is used today, the interface chamber or the submerged chamber. These chambers, however, have the disadvantage that they are limited in either their experimental or their physiological properties respectively. Here we present a new working principle for an *in vitro* chamber design which aims at combining the advantages of the classical designs whilst overcoming their disadvantages. This is achieved by using a semipermeable membrane on which the slice is placed. The membrane allows for a fast flow of artificial cerebrospinal fluid of up to at least 17 ml/min. Due to a Bernoulli effect, this high speed flow also causes a 64% increase in flow of solution across the membrane on which the slice rests. The fact that the membrane is transparent introduces the possibility of wide field inverted optical imaging to brain slice electrophysiology. The utility of this setup was demonstrated in the recording of local field potential, single cell and voltage sensitive dye imaging data simultaneously from an area smaller then 1/8 mm^2. The combination of all these features in the membrane chamber make it a versatile and promising device for many current and future *in vitro* applications, especially in the regard to optical imaging.

1. Introduction

In vitro brain slice experiments have the great advantage that they can be accurately controlled. Extracellular drug, ionic and modulatory concentrations can be precisely set and varied. Neuroanl networks in brain slices are limited to local connections only. Virtually any part of the brain can be accessed and targeted under visual guidance, and the *in vitro* preparation can be used in absence of anaesthetics, which can obscure the interpretation of data in many *in vivo* experimental situations.

At the same time however, *in vitro* studies are limited due to the simple fact that the brain has been reduced down to a slice. The physiology of the *in vitro* brain slice is maintained artificially, and the degree to which the 'normal' physiological state is recreated will determine the validity and quality of the data obtained from it. It is therefore important to ensure that the brain slice is kept under optimal conditions during *in vitro* experiments. The design of the chamber, in which the slice is maintained, is thus a pivotal factor in the design of any *in vitro* brain slice experiment. Here we present a new type of *in vitro* recording chamber that aims at providing improved physiological and experimental conditions in a simple, user friendly design.

1.1. Recording chambers

Countless alterations of the original brain slice recording chamber (Li and McIlwain, 1957) have been developed to improve recording conditions, and many laboratories design their own versions to meet their individual needs. However, when comparing various types of chambers, a significant degree of similarity can be seen in their basic desing. They tend to be modeled on either the interface chamber (also referred to as 'Oslo' or 'Haas' type chamber, Haas et al., 1979; Dingledine et al., 1980) or the submerged chamber (also referred to as perfusion or superfusion chamber, Croning and Haddad, 1998).

1.1.1. The interface chamber

In the interface chamber the brain slice lies on the interface of a liquid and a gaseous phase. Usually either a nylon mesh or some filter paper supports the slice allowing for oxygenated and temperature controlled artificial cerebrospinal fluid (aCSF) to supply the slice with salts and sugars from underneath. At the same time humidified oxygen (usually 95% O_2/5% CO_2) is provided to the slice from on top (Li and McIlwain, 1957; Gibson and McIlwain, 1965; Richards and Sercombe, 1970; Schwartzkroin, 1975; Knowles, 1985; Thiemann et al., 1986; Palovcik and Phillips, 1986; Matthies

* Corresponding author. Current address: California Institute of Technology, 216-76, 1200 E. California Blv., 91125 Pasadena, CA, United States. Tel.: +1 626 395 8962.
E-mail address: mrhill@caltech.edu (M.R.H. Hill).

0165-0270/$ – see front matter © 2010 Elsevier B.V. All rights reserved.
doi:10.1016/j.jneumeth.2010.10.024

et al., 1997). This basic principle is sometimes extended by the use of some type of wick for transporting aCSF to and from the slice (Haas et al., 1979; Kelso et al., 1983; Schurr et al., 1985; Dean and Boulant, 1988; Matthies et al., 1997). Another modification in one design is a second nylon mesh on top of the slice providing a thin film of aCSF between the slice and the oxygen (Tcheng and Gillette, 1996). The main advantage of the interface chamber is the high concentration of oxygen directly available to the slice. This allows for more realistic physiological recordings including *in vitro* recordings of network oscillations (Hájos et al., 2009).

The interface chamber however has some significant disadvantages. The two main ones being the fact that the slice can be compressed due to gravity which may change its physiology (Croning and Haddad, 1998) and that the turnover of aCSF is very slow (Reid et al., 1988; Zhang and Heinemann, 1992; Thomson et al., 2000; Wu et al., 2001; Hájos and Mody, 2009). Additionally, the upper surface of the slice is 'dry' (although in fact there is a thin film of solution due to meniscal and capillary forces). As a result it has a macroscopically uneven surface, which, depending on the aim of the experiment and the optics of the microscope, can be a disadvantage. In the case of wide field imaging, for example, the unevenness of the surface creates an inhomogeneous landscape of focus, refraction and reflection resulting in heavily compromised image quality.

1.1.2. The submerged chamber

In the submerged chamber the slice lies at the bottom of a continuously perfused pool of oxygenated aCSF. It is sometimes supported by a piece of filter paper or nylon mesh to facilitate perfusion, or it can be held in place by a small weight (a 'slice holddown', White et al., 1978; Scholfield, 1978; Nicoll and Alger, 1981; Koerner and Cotman, 1983; Zbicz and Weight, 1985; Sakmann et al., 1989; Fujii and Toita, 1991; Tominaga et al., 2000; Blake et al., 2007; Hájos and Mody, 2009). The main advantage of the submerged chamber is the high diffusion rate of bath-applied drugs into and out of the slice. The fact that the brain slices are fully submerged, also allows them to preserve their natural morphology even over long periods of experimentation (Croning and Haddad, 1998). Additionally, water immersion objectives allow for visualisation of individual neurons and accordingly guided patch clamp recordings (Sakmann et al., 1989; Edwards et al., 1989; Stuart et al., 1993). At the same time, wide field optics can also take advantage of the submerged setup. The meniscus of the aCSF in the submerged chamber provides an approximately flat surface allowing for high quality imaging. The main disadvantage of the submerged chamber is that the oxygen supply to the slice is limited by the liquid vector resulting in physiologically less ideal recording conditions.

1.2. Oxygen availability

There are two main strategies that are implemented in recording chamber designs to increase the supply of oxygen to the submerged brain slice. Either the flow rate of the aCSF is increased and the volume of the chamber is reduced, or the slice is suspended in the submerged chamber so that aCSF can diffuse into it from both sides as opposed to just from on top (Hájos and Mody, 2009). A recently introduced recording chamber combined both these advantages into its design, resulting in significantly improved slice physiology at flow rates of approx. 4–6 ml/min (Hájos et al., 2009; Hájos and Mody, 2009).

Beyond these two strategies there is however at least one more technique available for increasing oxygen availability to the slice: active flow. Here aCSF is actively 'pushed' or 'pulled' through the slice. The increased flow can be achieved by simply forcing aCSF through the slice or by more elaborate methods such as injecting it into the specimen with the help of microneedles (*e.g.* Koerner and Cotman, 1983; Choi et al., 2007). Besides the increased flow rate and the suspended slice design, the chamber presented in this study, additionally applies active flow to increase oxygen availability. The active flow in the new chamber is the direct result of a fast flow along the bottom surface of a semi-permeable membrane on which the slice rests. This fast flow creates a Bernoulli effect sucking aCSF through the membrane. The Bernoulli effect is expressed in Bernoulli's principle stating, that for an inviscid flow, an increase in speed of the fluid causes a decrease in pressure or a decrease in the fluid's potential energy:

$$\frac{v^2}{2} + \Psi + \frac{p}{\rho} = \text{constant} \quad (1)$$

where v is the flow speed, Ψ the gravitational potential, p the pressure and ρ is the density.

In the chamber both Ψ and ρ can be assumed to be constant. Therefore, with a high flow speed v of aCSF, a reduction in the pressure p can be achieved. As a result of the reduction of pressure, solution surrounding the fast flowing volume is sucked into its stream. Also, because the flow passes below the membrane, the suction is exerted across it, resulting in an active flow of aCSF through the membrane. This active flow across the membrane will suck the slice down onto the membrane and increase perfusion of the bottom surface of the slice. This could also potentially lead to a higher turnover of solution within the slice.

1.3. Optical improvements

The new chamber was also designed to feature improved optical imaging properties. Suspending a slice on mesh can lead to an uneven topography where the slice 'hangs' in between the threads. This can lead to an uneven focus when using wide field optics with high numerical apertures. Filter membranes (Tominaga et al., 2000), on the other hand, can be too opaque to allow for inverted imaging and their stickiness will compromise the imaged surface of the slice. In contrast, the semipermeable membrane used here is flat, smooth and inert, and can therefore provide more optimal conditions to support the slice. The membrane is also transparent. This feature introduces a completely new possibility to large scale *in vitro* optical imaging of brain slices: unhindered inverted imaging. Inverted optical imaging has the great advantage that it leaves the upper surface of the slice free for additional experimental devices.

All these points were taken into consideration when designing the new *in vitro* recording chamber. With its transparent semipermeable membrane and its use of the Bernoulli effect, this chamber is based on very different working principles compared to the interface and submerged chambers. To distinguish it from these two classical designs, this new, third type of *in vitro* recording chamber is referred to as the *membrane chamber*.

2. Materials and methods

The main body of the membrane chamber presented here was constructed from two Perspex plates. Milled grooves in the upper of the two plates formed tunnels that were closed off once the two plates were assembled together. These tunnels were used for aCSF transport and for the thermistor and the reference electrode (red and yellow wires in Fig. 1a). A thin film of silicon between the two plates provided a good seal. On top of this base plate a small Perspex construction provided the walls around the individual sections of the chamber. These walls were adhered with silicon and could easily be removed for cleaning and maintenance (see supplementary figure S1 for details on the construction of the chamber).

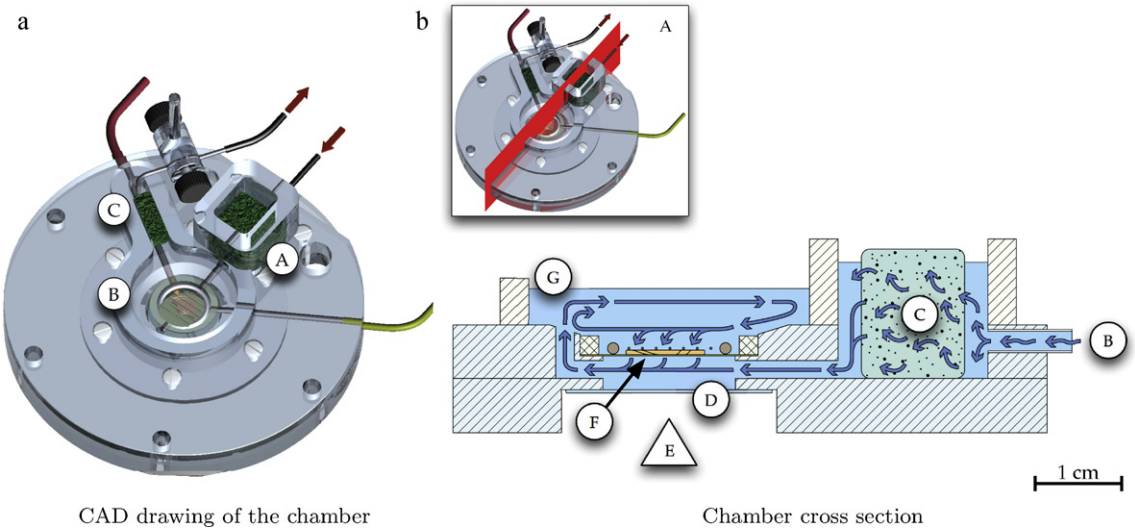

Fig. 1. Overview of the chamber design. The fully assembled chamber (a) consisted of three main parts: (A) the pre-chamber, into which the solution was injected, (B) the recording chamber proper, which was made up of the infra- and the supra-chamber and (C) the post-chamber, from where the solution was sucked out. A cross section of the chamber (b) along the red plane (inset A) shows the flow of solution through the chamber. The solution was injected into the pre-chamber by a peristaltic pump (B) resulting in short, uneven pulses (arrows from B to C). In the pre-chamber a block of porous polyester wool (C) induced turbulence into the flow resulting in a more even laminar flow (arrows from C to D). This fast laminar flow then passed through the infra-chamber (D) along the bottom surface of the membrane carrying the brain slice (F). As the solution passed under the membrane at high speed, it exerted a Bernoulli effect, sucking solution through the membrane (indicated by arrows). The infra-chamber was sealed from below by a 20 mm diameter coverslip which also functioned as a window onto the slice in the camera's line of view (E). The solution was then passed into the supra-chamber (G) where it flowed into the post-chamber, and was finally sucked out by the peristaltic pump (not visible in this cross section). (For interpretation of the references to colour in this figure legend, the reader is referred to the web version of the article.)

2.1. Particle imaging velocimetry

Particle imaging velocimetry (PIV, Adrian, 1991) was used to record the speeds and dynamics of the solution inside the chamber. In the pre-chamber the solution was seeded with 40 μl of an aqueous suspension of micro particles just as imaging commenced. The solution used had a 5% solid content of polystyrene based dark red particles with a diameter of 100 μm (Sigma–Aldich™ Ltd, Dorset, UK). PIV videos were recorded with the Brainvision™ MICAM02 system (Brainvision™ Ltd, Tokyo, JP; SciMedia™ Ltd, Costa Mesa, USA). All trials were acquired with a frame rate of 125 Hz over a period of 10 s. The acquired PIV data was analysed with a custom written Matlab™ (MathWorks Ltd., Cambridge, UK) script based on the mpiv toolbox (mpiv – Matlab PIV toolbox, version 0.965, Mori and Chang, 2006).

2.2. Measuring the Bernoulli effect

An experiment in two parts was designed to measure the presence and degree of a Bernoulli effect across the membrane. In the first part, the chamber was set up as usual using a semipermeable membrane, but with water instead of aCSF circulating at 16.95 ml/min. Tubing was placed into the connection between the infra- and supra-chamber (Fig. 1b) so that the water could flow through the infra-chamber and out of the system without going through the supra-chamber. As a result the upper surface of the membrane stayed dry. Onto this 400 μl of 0.25 g/ml tartrazine were placed (Sigma–Aldich™ Ltd, Dorset, UK). The water was then run through the infra-chamber for 29.5 min and the output (0.5 l) was collected in a measuring cylinder. At the end of the experiment samples from the tartrazine solution on the membrane and from the collected water were taken for further analysis. The two samples were called active input and active output respectively; the term 'active' referring to the fact that an active flow of the tartrazine across the membrane was expected due to a Bernoulli effect.

In the second part of the experiment measuring cylinders were filled with 0.5 l of water and placed in a room with minimal air circulation to prevent any disturbance of the solution. Membranes were then placed onto the surface of the water, where they floated stably. Onto these membranes 400 μl of 0.25 g/ml tartrazine were placed. The tartrazine was allowed to diffuse across the membrane passively for 29.5 min. After the experiment ended passive input and passive output samples were also collected for further analysis. The four collected samples were diluted as necessary and analysed in a microplate reader at 405 nm (υ_{max} Kinetic Microplate Reader, Molecular Devices™, MDS Analytical Technologies Inc., USA). The measured absorbance was then compared with a dilution series to calculate the final tartrazine concentrations in the input and output solutions under the two different conditions (active flow *vs*. passive diffusion).

2.3. Solution replacement timecourse

An experiment was conducted to measure the time it takes for a solution in the chamber to be completely replaced by another solution. For this experiment water was run through the chamber, which was set up as usual. The clear water input was then replaced by a yellow solution of tartrazine. Whilst the tartrazine was running through the chamber and replacing the clear water, samples were taken from the outflow of the chamber at 3 s intervals. The timecourse of the solution replacement was measured on a microplate reader and plotted against time in Matlab™.

2.4. Slice survival

Hippocampal local field potential (LFP) recordings were used to measure the longevity of slices in the membrane chamber. All experiments were conducted in accordance with the Animals (Scientific Procedures) Act 1986 (UK). Adult male CB57BL/6 mice (Harlan Laboratories™, Bicester, UK) were killed with an overdose of anaesthetic (IsoFlo™, Abbott™ Animal Health, Illinois, USA). The brain was carefully removed and cooled down in aCSF at 0 °C for approximately 1–2 min. aCSF was prepared and stored as two separate stock solutions with the final solution containing: 124 mM

NaCl, 5 mM KCl, 1.25 mM NaH_2PO_4, 1.25 mM $MgSO_4$, 2 mM $CaCl_2$, 10 mM glucose and 22 mM $NaHCO_3$ at pH 7.4. When harvesting hippocampal slices, a dorsal piece of cortex was cut from each hemisphere horizontally and the revealed surface glued to the vibratome stage. 400 μm thick slices were then sectioned with a vibratome (VT 1000S, Leica™ Microsystems, Milton Keynes, UK) and transferred to oxygenated aCSF, slowly heated up to 32 °C, and incubated until the actual experiment commenced.

After incubation for 60–90 min, the slices were moved to the actual recording chamber for experimentation (only one slice per experiment). In the chamber the slice was orientated so that the region of interest was in the centre of the chamber where the solution turnover was highest. A concentric bipolar tungsten micro electrode (CBARC75, FHC™, Bowdoin, USA) was then placed into the Schaffer collaterals within the region of the CA2/CA3 boundary. A monopolar tungsten microelectrode (UEWMEFSEBN3M 10/60/0, FHC™, Bowdoin, USA) was used for recording the LFP within the stratum radiatum of the CA1. The slices were left to equilibrate in the recording chamber with the electrodes in place for 20 min prior to experimenting. Hippocampal slices were stimulated every 15 min with a single pulse of 0.2 ms over a period of 16 h. The stimulation current was set to the value needed to evoke a half-maximal LFP response amplitude. The recorded signals were amplified 10× in a Neuro Data IR-283 amplifier (Cygnus Technology™, Delaware Water Gap, USA) and amplified again 100× in an in-house custom made amplifier and low pass filter module (1 kHz, Preston, M, Department of Pharmacology, Oxford, UK).

2.5. Simultaneous recordings

Simultaneous recordings of voltage sensitive dye imagaing (VSDI), local field potential (LFP) and single cell data were acquired in somatosensory thalamocortical slices. These were harvested in the same way as the hippocampal slices but the brains were blocked according to Agmon and Connors (1991). The stimulating electrode was placed in the VPM of the thalamus and the LFP recording electrode was positioned in the barrel cortex. A whole-cell patch-clamp electrode was also placed in the barrel cortex. Patch-clamp electrodes were pulled from standard-wall borosilicate glass tubing. The electrodes were filled with a solution containing 110 mM potassium gluconate, 40 mM 4-[2-hydroxyethyl]piperazine-1-ethanesulfonic acid (HEPES), 4 mM NaCl, 4 mM ATP-Mg and 0.3 mM GTP. The solution was adjusted to pH 7.1 and an osmolarity of 290. Patch-clamp electrodes were placed into the barrel cortex blindly (Castaneda-Castellanos et al., 2006). The data was amplified in an Axopatch 200A patch-clamp amplifier (Molecular Devices™, Sunnyvale, USA). All LFP and single cell data was recorded with the Signal™ software in combination with the Micro 1401 mkII AD/DA converter (both from Cambridge Electronic Design™, Cambridge, UK).

Di-4-ANEPPS (Invitrogen™, Molecular Probes™, Paisley, UK) voltage sensitive dye stock solution was made up at a 6.93 mM in 7% (v/v) cremophore EL (Sigma–Aldich™ Ltd, Dorset, UK) in DMSO. The final dye solution was made up on the day of experimentation by adding 50% (v/v) oxygenated aCSF to foetal bovine serum with a total resulting volume of 1.5 ml. To this 80 μl di-4-ANEPPS stock solution were added resulting in a final concentration of 0.35 mM. The final dye solution was kept in a 5 ml eppendorf tube topped up with 95% O_2/5% CO_2 and vortexed for 3 min to ensure adequate oxygenation before application to the slices.

After incubation in oxygenated aCSF, the brain slices were placed on filter paper submerged in oxygenated di-4-ANEPPS solution. They were protected from light at room temperature for 30 min. After dye internalisation slices were rinsed with aCSF and returned to the incubation chamber. This was then placed into a light protected water bath where slices were slowly warmed back up to 32 °C until transferal into the actual recording chamber.

VSDI images were acquired with a Brainvision™ MICAM02 system (Brainvision™ Ltd, Tokyo, JP, SciMedia™ Ltd, Costa Mesa, USA) and an in-house custom made inverted microscope (Hill, M.R.H., Department of Pharmacology, Oxford, UK). VSDI data was acquired with the Brainvision Analyzer software (Brainvision™ Ltd, Tokyo, JP, SciMedia™ Ltd, Costa Mesa, USA) and processed in Matlab™.

3. Results

3.1. Fluid dynamics

The membrane chamber consisted of three main sections (Fig. 1a). In the first section, the *pre-chamber* (Section 3.1.1), a thin stainless steel tube formed a connector for silicone tubing. Through this inlet aCSF was injected into the pre-chamber by a peristaltic pump. From the pre-chamber a small tunnel allowed the aCSF to flow to the *recording chamber proper* (Section 3.1.2) where the brain slice was incubated for recording. The recording chamber proper was continuous with the *post-chamber* (Section 3.1.3) where the aCSF was sucked up again by a small stainless steel tip.

3.1.1. Pre-chamber

The pre-chamber's inlet was set at a different height from the connection to the recording chamber proper (Fig. 1b). This ensured that any pressure waves originating from the peristaltic movement of the aCSF pump could not expand directly into the recording chamber proper. The pre-chamber was designed to be quite large, allowing any pressure differences to equilibrate in this reservoir before reaching the recording chamber proper. The peristaltic motion of the aCSF was counteracted further by passing it through porous polyester wool obtained from a polyester scouring pad. This induced a large amount of turbulence, reducing the vibrations caused by the aCSF flow and resulting in a laminar flow from the pre-chamber to the recording chamber proper.

Besides reducing vibrations, the porous polyester wool also provided a large amount of rough surface area in the aCSF just before the recording chamber proper. This surface area facilitated the formation of bubbles, which are inevitable in a flow of warm aCSF in an environment at room temperature. The presence of the porous polyester wool allowed bubbles to form within the pre-chamber, instead of in the recording chamber proper where they would otherwise interfere with data acquisition.

3.1.2. Recording chamber proper

The recording chamber proper was the core of the whole design and consisted of two sub sections, the *infra-chamber* and the *supra-chamber* (Fig. 1b). The laminar flow of aCSF from the pre-chamber flowed through the infra-chamber and was then tunnelled into the supra-chamber. The infra-chamber was designed in such a way that this flow of aCSF ran directly along the under side of a semi-permeable membrane separating the infra-chamber from the supra-chamber (supplementary figure S2c).

Infra-chamber: From underneath the infra-chamber was sealed by a glass coversilp (supplemetary figure S2d). As a result of this overall design, the brain slice lay only on the transparent membrane followed by 2 mm of aCSF and the coverslip. This created good conditions for optical imaging. The semipermeable membrane provided a transparent and flat surface, allowing nutrients to flow through whilst gently flattening the slice's under side. The membrane and the coverslip could easily be replaced to guarantee a clean optical pathway. However, as the flow of aCSF crossed the optical path in the infra-chamber, particles in the aCSF could interfere with imaging. To prevent this, all aCSF was filtered with an

in-line filter system just before entering the pre-chamber (in-line polysulfone filter holder, Fisher Scientific™, Loughborough, UK).

Supra-chamber: From the infra-chamber the aCSF flowed into the supra-chamber. The input into the supra-chamber pointed upwards creating a skewed convection cell within the supra-chamber. This convection cell gently provided the upper side of the slice with aCSF from all sides uniformly. As a result, uneven currents on the upper surface of the slice were minimized allowing it to rest at the bottom of the supra-chamber quietly. The fluid environment around the slice was so stable – even at high flow rates – that VSDI could be conducted without the need of a slice hold-down or a slice glue.

3.1.3. Post-chamber

The round supra-chamber was continuous with the narrow post-chamber exiting it from one side (Fig. 1a). At the far end of the post-chamber a height-adjustable suction tip was lowered into the aCSF. This suction tip was sealed off at the end and only opened through a thin slit along its side. This slit broke the meniscus of the solution resulting in an overall smoother suction (the design of this suction tip principle can also be seen in other setups). However, even with this suction tip, a certain amount of vibration due to the suction remains. A small block of porous polyester wool was inserted into the post-chamber between the suction tip and the supra-chamber to prevent this vibration from spreading back into the supra-chamber and interfering with the slice.

3.2. Membranes

Membranes were produced by initially soaking dialysis membrane (SnakeSkin Pleated Dialysis Tubing, MWCO 10,000, Perbio Science™ Ltd, Cramlington, UK) in distilled water for approx. 2 min. After soaking the membrane became soft and stretchable. It was then carefully stretched over a hard plastic tube and held in place with a rubber ring (supplementary figure S2a). A 2 mm thick Perspex ring with an inner diameter of 15 mm was then glued onto the stretched membrane. After approx. 1 min the rubber ring could be removed and the taught membrane fixed firmly to the Perspex ring was gently freed from the plastic tube. The membrane was finalised by trimming off any remaining material around the edge of the Perspex ring with a razor blade (supplementary figure S2b). Production of membranes took about 5 min per unit. Fresh membranes were prepared for each experiment to guarantee a clean environment for the slice, free pores within the membrane and a clear optical pathway for imaging.

3.3. Flow speed

The speed of the flow inside the infra-chamber as well as its dynamics were measured with particle image velocimetry. At a flow rate of 13.5 ml/min the average velocity in the centre of the chamber was measured to be $\bar{m} = 60.56$ mm/s (sem = 12.48). At a flow rate of 17 ml/min the measured velocity was $\bar{m} = 189.32$ mm/s (sem = 28.31), $n = 3$ (Fig. 2). The flow was found to be laminar along the flow direction through the centre of the chamber. Only at flow rates as high as 25 ml/min did it start to break down into short-lived local turbulence. This, however, was still small enough not to affect the basic working design and principle. At the other end of the infra-chamber, where the aCSF flowed into the supra-chamber, most of the aCSF continued straight on along this path. Only a small amount fanned out along the walls and circulated back towards the infra-chamber inlet (Fig. 2a).

A velocimetry quiver map was drawn to get better insight into the distribution of the flow velocities. The main fast flow across the centre of the infra-chamber was found to be laminar throughout (Fig. 2b). This area of high speed flow had a diameter of over 3 mm and a length of most of the 15 mm chamber diameter. As a result, a large part of the membrane area (approx. 4 mm × 10 mm) could be used to create an active flow across the membrane. At the same time, the areas to either side of this active flow zone were still perfused with a relatively high turnover. In view of these measurements the Bernoulli effect could therefore be assumed to only take place to any relevant degree within the active zone in the centre of the membrane.

3.4. Bernoulli effect

The flow of solution through the membrane was recorded to confirm the presence, and measure the degree, of a Bernoulli effect (Fig. 3). In an active flow paradigm 0.4 ml of 0.25 g/ml (467.85 μM) tartrazine solution (input) were placed on top of a membrane and 0.5 l of water was washed through the chamber at 16.95 ml/min (output). In comparison, membranes loaded in the same way were left to float on 0.5 l of water for 29.5 min (passive diffu-

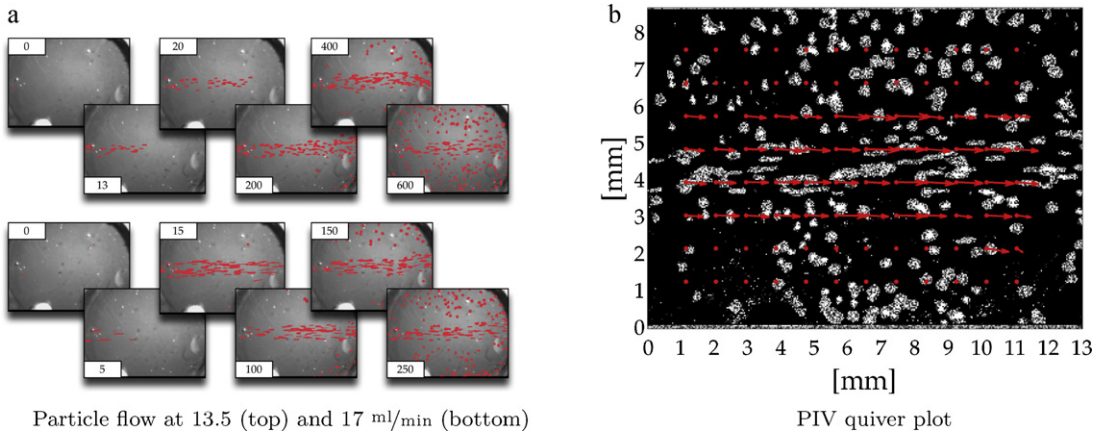

Fig. 2. Fluid dynamics inside the infra-chamber. Particle imaging velocimetry was used to visualise the flow of aCSF in the infra chamber at two different flow rates (a). At both speeds a clear stream of red particles could be seen along the central axis of the chamber. Only after a while did the particles begin to fan out along the walls and back to the inlet. At the lower flow rate of 13.5 ml/min this occurred about 200 ms after entry of the first particle into the chamber. At the higher flow rate of 17 ml/min the fanning out already occurred after 100 ms. (b) A representative picture of the particles in the infra-chamber is shown here in black and white. On this background red arrows represent the mean maximal velocity in that region measured over 4 s at a flow rate of 13.5 ml/min. A distinct homogeneous field of high-velocity vectors can be seen in an area of about 4 mm × 10 mm in the centre of the chamber. (For interpretation of the references to colour in this figure legend, the reader is referred to the web version of the article.)

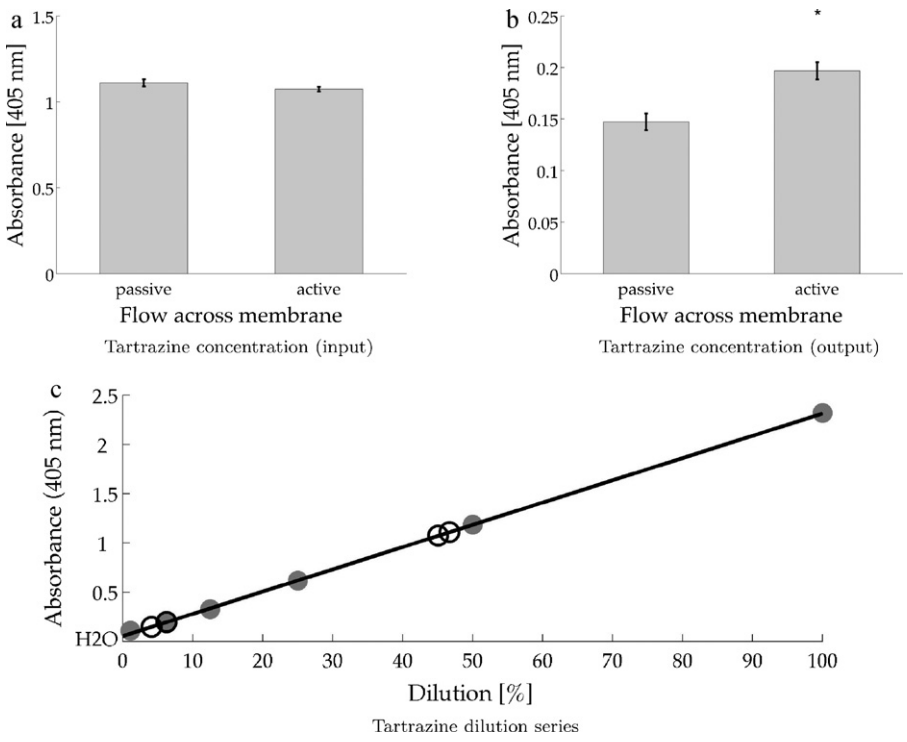

Fig. 3. Measuring the Bernoulli effect. Comparison of the absorbance (1/32,000 × original concentration) of the tartrazine input at the end of the experiment (a) with a reference dilution series (100% = 1/32,000 × input concentration, c) showed that the input concentration was diluted to 46.69% under passive dilution and to 45.09% under active flow (higher pair of circles in c). A two sided *t*-test (a) showed no significant difference between these two dilutions ($p = 0.1778$). As a result the actual mean input concentration in the passive diffusion experiment was 0.183 g/ml, and in the active flow 0.181 g/ml. After measurement of the output absorbance (b) and comparison to the reference (lower pair of circles in c) under consideration of the calculated *mean* input concentrations, the total amount of solution that diffused across the membrane into the output was measured to be 0.871 μl under passive diffusion and 1.352 μl under active flow. A two sided *t*-test (b) showed these concentrations to be significantly different ($p = 0.0054$), $n = 6$; error bars show the sem, grey markers in c show the actual measured absorbances, the black line in c is a best linear fit to the actual measured absorbances ($y = 0.022596x + 0.054812$, norm of residuals = 0.034).

sion). Due to the high osmotic gradient between the tartrazine and the water, the original input solution got diluted during the course of the experiment. The final concentrations in the input after 29.5 min were 0.1127 g/ml (sem = 0.0015) under active flow and 0.1167 g/ml (sem = 0.0023) under passive diffusion (Fig. 3a). As a result, the mean tartrazine concentration was calculated to be $\bar{m} = 0.181$ g/ml (sem = 0.00076) as the passive input and $\bar{m} = 0.183$ g/ml (sem = 0.0012) as the active input. From these corrected input concentrations the total volume of solution flowing through the membrane was calculated as 1.352 μl (active, sem = 0.079) and 0.871 μl (passive, sem = 0.077). Subtracting the two from each other revealed the total amount of solution sucked through the membrane as a direct result of the Bernoulli effect. This was 0.48 μl (sem = 0.112) or 64% more flow of solution due to the Bernoulli effect ($n = 6$).

3.5. Solution replacement time

A great advantage of high flow rates for *in vitro* experimentation is the fact that drugs can be washed in and out of the chamber and the brain slice much faster. The time used to completely replace one solution with another within this membrane chamber was measured at both 13 and at 17 ml/min. At 13 ml/min all the solution had been exchange after 150 s, at 17 ml/min the turnover was in the range of 110 s ($n = 3$, Fig. 4a).

3.6. Slice viability

The most important parameter in any *in vitro* slice recording chamber will always be the viability of tissue. A good measurement for this is the survival time of the slice. The longer one is able to record stable responses, the more comfortable one can be about working with physiologically stable specimens. To measure slice viability, LFPs in the hippocampus were measured every 30 min over a total period of 16 h. The LFP signal stayed very stable over the whole recording period. After 16 h the response amplitude was still in the same range as at the beginning of the experiment (around −100 μV). The measured LFP signal amplitudes were −97.05 (sem = 60.85) at the start of the experiment and −108.2 (sem = 74.8) at the end, $n = 3$ (Fig. 4b).

3.7. Data acquisition

Single cell recordings were attempted, to test whether they could be achieve and maintained for a significant period of time inside the membrane chamber. As this method is very sensitive to movements and vibrations of any kind, it was used to test the chamber's overall mechanical stability as well as its behaviour at the level of microscopic vibrations. Cells could generally be patched easily in the membrane chamber and could be maintained for more then 1 h ($n = 6$, Fig. 5b).

From the findings reported here we thus conclude that the chamber presented itself as a stable and effective setup for *in vitro* imaging and electrophysiology. Furthermore, by imaging from underneath and inserting electrodes from on top, VSDI, LFP and single cell data could be recorded from the same location simultaneously (Fig. 5).

4. Discussion

The membrane chamber presented here was used extensively in electrophysiological experiments over a period of three years

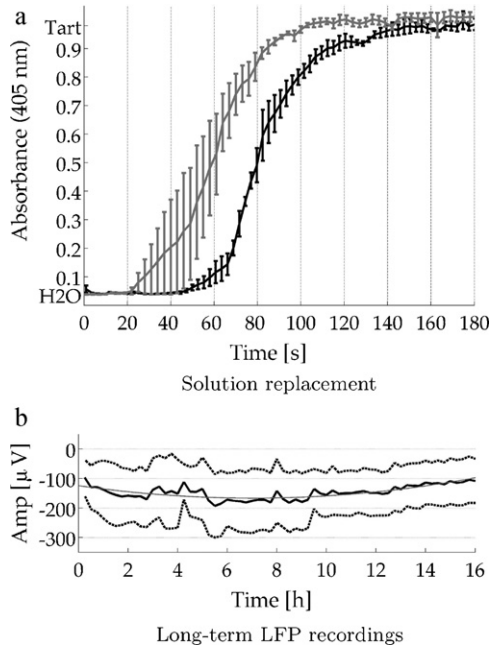

Fig. 4. Solution replacement time and slice survival. At a high flow rate of 17 ml/min (grey line in a) it takes approximately 110 s to replace all of solution A (H_2O) with solution B (tartrazine), $n = 3$. At the lower flow rate of 13.5 ml/min, the solution replacement time is in the range of 150 s (black line in a), $n = 3$. The solution replacement time was measured as the time it takes for the absorbance to change from that of H_2O to that of tartrazine; error bars show the sem, x-axis error bars are <1 s and are therefore not visible. The LFP signal in the CA1 (b) stays relatively stable over the course of 16 h with an initial response amplitude (Amp) of −97.05 μV and a final response amplitude of −108.2 μV after 16 h. Quadratic curve fitting (grey line in b) however still reveals a slight increase in LFP response amplitude over the first 7 h and a corresponding decrease during the remaining 9 h (note the negative y-axis scale), $n = 3$; dashed lines represent the sem.

(upcoming publications). During this time it proved to be a reliable and user friendly laboratory device. The removable membranes, glass coverslip seals and walls allowed the device to be easily cleaned and maintained. The chamber was also found to work well for optical imaging. The inverted setup meant that slices inside the chamber were automatically in focus and imaging could commence without delay. Additionally, the slices were easily accessible from on top for additional electrophysiological measurements. As a result of this design, working with the membrane chamber proved to be very efficient.

4.1. The Bernoulli effect

The Bernoulli effect could clearly be demonstrated in the membrane chamber, the respective experiment measured the presence and the relative magnitude of this effect. However, the final amount of solution flowing accross the membrane may actually be higher in an experimental setup with a brain slice.

Over the timecourse of the experiment more then 200 μl of water flowed across the membrane from the infra-chamber into the supra-chamber. The flow is believed not to have been caused by a difference in the overall pressure between the two chambers as they were both held at atmospheric pressure. Rather, this flow, which moves in the opposite direction to the Bernoulli effect, was most probably caused by the strong osmotic gradient due to the high concentration of the input solution.

Due to the simple linear nature of the Bernoulli effect (Eq. (1)) the recorded generic values remain valid even in the presence of the strong suction in the opposite direction. As a result, it is safe to conclude that in the membrane chamber the Bernoulli effect leads to a 64% increase of flow across the membrane. The final amount of solution that this may translate into in a real experiment, where there is no osmotic gradient, will however also depend on various additional factors such as the molecular weight cutoff of the membrane and the area and thickness of the brain slice resting on it.

Even so, in the current design, the absolute amount of flow of aCSF through the membrane will, in general, still be small. Indeed it is unlikely to have an effect on the actual turnover of oxygen within the slice. Thus, the main advantage of the Bernoulli effect in this version of the membrane chamber lies in the fact that it causes suction *underneath* the slice, not in that it causes active flow *through* the slice. The advantage of this suction is that it holds the slice stably at the bottom of the chamber without the need of a slice hold-down and that it will cause a higher turnover of aCSF in the space between the slice and the membrane facilitating perfusion of the bottom surface of the slice.

In theory, the *in vitro* brain slice can be regarded as porous, therefore suction on one side will result in a flow of solution through it. The fact that the membrane chamber can cause such suction is encouraging. In this respect the current findings are also to be regarded as a proof of concept, which will hopefully lead to further develpements in this vein.

4.2. Slice physiology

The physiological advantages of the membrane chamber were confirmed by the recording of stable LFPs over a period of 16 h. It has, however, been reported that the LFP – at least in organotypic slice cultures – is not a very oxygen sensitive parameter (Huchzermeyer et al., 2008). This means that the LFPs probably cannot be used to report the effects of any short term oxygen fluctuations. In long-term experiments, such as the ones presented here, however, it remains a valid measurement as a lack of oxygen will eventually lead to an increase in cell death resulting in a reduction of the LFP amplitude.

The survival time of brain slices is often used as an argument for the quality of a recording chamber. However, comparison of various chambers on the basis of this parameter is difficult as such claims are rarely experimentally substantiated. Direct comparison is further constrained by the fact that different parameters, protocols and specimens are used in the various studies. For different types of submerged chambers the slice survival time has been reported to be in the range of 10–12 h (White et al., 1978; Nicoll and Alger, 1981; Zbicz and Weight, 1985) and up to 16 h (albeit in only two cells, Scholfield, 1978). In interface chambers a similar range has been described (Richards and Sercombe, 1970; Knowles, 1985; Thiemann et al., 1986; Matthies et al., 1997), with some reports reaching up to 30 h (Palovcik and Phillips, 1986) and even 70 h (Tcheng and Gillette, 1996).

4.3. Outlook

Although the membranes used in the current study displayed many advantages for *in vitro* electrophysiology, there is still room for improvement. An ideal membrane has pores that are as large as possible for maximal flow of solution but at the same time it must remain transparent to the relevant wavelenghts for optical imaging. Further research to optimize membrane properties would be beneficial to the improvement of future recording conditions.

In the current study it was also observed, that polylysine (Sigma–Aldich™ Ltd, Dorset, UK) sticks to the membranes. In some applications this may prove to be a better way to hold slices in place. For example, if experimental interest only concerns the hippocampus, then the surrounding cortex and thalamus could be glued to the membrane. Whilst the polylysine would block the membrane

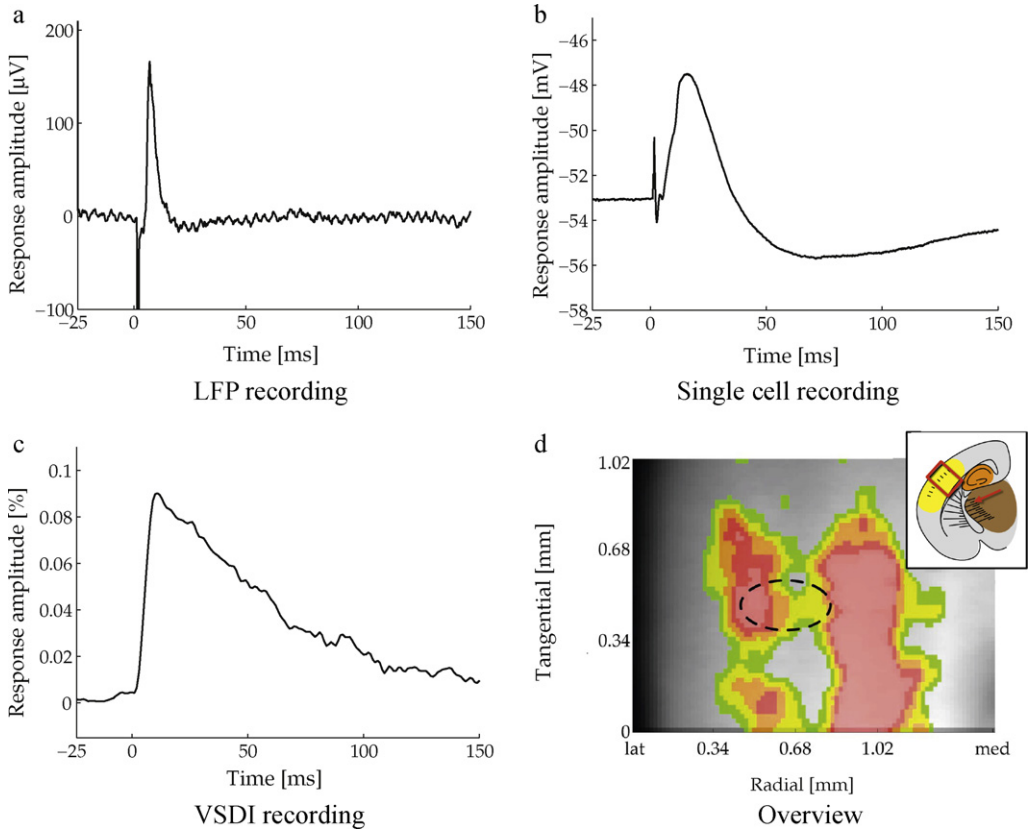

Fig. 5. Simultaneous electrophysiology and VSDI. To display one of the advantages of the membrane chamber, LFP (a), single cell (b) and VSDI (c) data was recorded simultaneously from the same location. Whilst the two respective recording electrodes were inserted into the slice from on top, the VSD response was recorded from underneath the slice. Even though all data was acquired from within an area of <1/8 mm^2 (dashed line in c), the recording electrodes do not obstruct the line of view of the VSDI. In the overview (d) the cortex can be seen in the black and white background image with the pia lateral (lat, black edge) and the sub cortical white matter medial. On top of this the VSDI signal is shown in colour – un-affected by the recording electrodes lying on the other side of the slice (warmer colours from green through yellow to red represent higher VSDI response amplitudes). The single cell patch-clamp recordings (b) were found to be stable and could be maintained for over 1 h at a time, $n = 6$. The inset in (d) shows the recording area (red rectangle) and the stimulation site (red arrow) in relation to the barrel cortex (yellow), the hippocampus (orange) and the thalamus (brown). (For interpretation of the references to colour in this figure legend, the reader is referred to the web version of the article.)

and render it useless in these areas, the hippocampus would still be actively perfused from both sides and at the same time held in place firmly.

Beyond this, further membrane adjustments may be considered for specific types of experiments. For example electrodes could be woven into membranes or membranes could be printed with grids or measurement bars. It may even be possible to print integrated circuits and electronic interfaces for bionic experiments. It would also be interesting to see how well the membrane chamber might be suited for other types of experiments such as imaging of cardiac specimens, organotypic slices or even cell cultures grown directly on transparent, semipermeable membranes.

Besides these manipulations of the membranes, the actual chamber might also be altered for specific applications. For example, aCSF could be removed directly from the tube leading to the supra-chamber. In the supra-chamber the slice would then be left to rest on the membrane surrounded by a small amount of aCSF. Whilst this would remain stationary, the flow of aCSF underneath the membrane and an additional source of oxygen from on top could keep it fresh, thus simulating the classical interface chamber design. In this way the membrane chamber could be used for very different types of *in vitro* brain slice experiments.

In conclusion, the membrane chamber introduces the possibility of inverted optical imaging to *in vitro* slice electrophysiology. The fast flow of aCSF in the chamber also allows for high oxygen and drug turnover, and the creation of a Bernoulli effect. These advantages, together with the user-friendly and versatile design, make the membrane chamber a valuable research tool, that can facilitate many diverse *in vitro* electrophysiological applications.

Conflict of interest

M.R.H. Hill declares conflict of interest with current development of a commercial application of the membrane chamber by Scientific Systems Design Inc, Mississauga, Ontario, Canada.

Acknowledgements

The authors would like to thank Matthias Furler for providing the CAD drawings, Dr. Ole Paulsen, Dr. Carl Petersen and Dr. Maria Carroll for valuable feedback as well as Dr. Christof Koch for his support. The research was financially supported by the Swiss Life Foundation, the Swiss Study Foundation and the Daniel Falkner Research Grant.

Appendix A. Supplementary data

Supplementary data associated with this article can be found, in the online version, at doi:10.1016/j.jneumeth.2010.10.024.

References

Adrian RJ. Particle-imaging techniques for experimental fluid-mechanics. Annu Rev Fluid Mech 1991;23:261.

Agmon A, Connors B. Thalamocortical responses of mouse somatosensory (barrel) cortex in vitro. Neuroscience 1991;41(2–3):365–79.
Blake AJ, Pearce TM, Rao NS, Johnson SM, Williams JC. Multilayer pdms microfluidic chamber for controlling brain slice microenvironment. Lab Chip 2007;7(7):842–9.
Castaneda-Castellanos D, Flint A, Kriegstein A. Blind patch clamp recordings in embryonic and adult mammalian brain slices. Nat Protoc 2006;1(2): 532–42.
Choi Y, McClain MA, LaPlaca MC, Frazier AB, Allen MG. Three dimensional mems microfluidic perfusion system for thick brain slice cultures. Biomed Microdevices 2007;9(1):7–13.
Croning M, Haddad G. Comparison of brain slice chamber designs for investigations of oxygen deprivation in vitro. J Neurosci Methods 1998;81(1–2): 103–11.
Dean JB, Boulant JA. A diencephalic slice preparation and chamber for studying neuronal thermosensitivity. J Neurosci Methods 1988;23(3):225–32.
Dingledine R, Dodd J, Kelly J. The in vitro brain slice as a useful neurophysiological preparation for intracellular recording. J Neurosci Methods 1980.
Edwards FA, Konnerth A, Sakmann B, Takahashi T. A thin slice preparation for patch clamp recordings from neurones of the mammalian central nervous system. Pflugers Arch 1989;414(5):600–12.
Fujii T, Toita K. A method for simultaneous recording of electrical activities and spectrophotometric signals from brain slice preparations in vitro. Pflugers Arch 1991;419(2):205–8.
Gibson I, McIlwain H. Continuous recordings of changes in membrane potential in mammalian cerebral tissues in vitro; recovery after depolarization by added substances. J Physiol 1965;176:261–83.
Haas H, Schaerer B, Vosmansky M. A simple perfusion chamber for the study of nervous tissue slices in vitro. J Neurosci Methods 1979;1(4):323–5.
Hájos N, Ellender TJ, Zemankovics R, Mann EO, Exley R, Cragg SJ, Freund TF, Paulsen O. Maintaining network activity in submerged hippocampal slices: importance of oxygen supply. Eur J Neurosci 2009;29(2):319–27.
Hájos N, Mody I. Establishing a physiological environment for visualized in vitro brain slice recordings by increasing oxygen supply and modifying acsf content. J Neurosci Methods 2009;183(2):107–13.
Huchzermeyer C, Albus K, Gabriel H-J, Otáhal J, Taubenberger N, Heinemann U, Kovács R, Kann O. Gamma oscillations and spontaneous network activity in the hippocampus are highly sensitive to decreases in po2 and concomitant changes in mitochondrial redox state. J Neurosci 2008;28(5):1153–62.
Kelso SR, Nelson DO, Silva NL, Boulant JA. A slice chamber for intracellular and extracellular recording during continuous perfusion. Brain Res Bull 1983;10(6):853–7.
Knowles W. A portable in vitro brain slice chamber. J Neurosci Methods 1985;14(3):187–92.
Koerner JF, Cotman CW. A microperfusion chamber for brain slice pharmacology. J Neurosci Methods 1983;7(3):243–51.
Li C, McIlwain H. Maintenance of resting membrane potentials in slices of mammalian cerebral cortex and other tissues in vitro. J Physiol (Lond) 1957;139(2):178–90.
Matthies H, Schulz S, Thiemann W, Siemer H, Schmidt H, Krug M, Höllt V. Design of a multiple slice interface chamber and application for resolving the temporal pattern of creb phosphorylation in hippocampal long-term potentiation. J Neurosci Methods 1997;78(1–2):173–9.
Nicoll RA, Alger BE. A simple chamber for recording from submerged brain slices. J Neurosci Methods 1981;4(2):153–6.
Palovcik RA, Phillips MI. A constant perfusion slice chamber for stable recording during the addition of drugs. J Neurosci Methods 1986;17(2–3):129–39.
Reid KH, Edmonds HL, Schurr A, Tseng MT, West CA. Pitfalls in the use of brain slices. Prog Neurobiol 1988;31(1):1–18.
Richards C, Sercombe R. Calcium, magnesium and the electrical activity of guinea-pig olfactory coex in vitro. J Physiol 1970;211(3):571–84.
Sakmann B, Edwards F, Konnerth A, Takahashi T. Patch clamp techniques used for studying synaptic transmission in slices of mammalian brain. Q J Exp Physiol (Cambridge, England) 1989;74(7):1107–18.
Scholfield C. Electrical properties of neurones in the olfactory cortex slice in vitro. J Physiol 1978;275:535–46.
Schurr A, Reid KH, Tseng MT, Edmonds HL, Rigor BM. A dual chamber for comparative studies using the brain slice preparation. Comp Biochem Physiol A Comp Physiol 1985;82(3):701–4.
Schwartzkroin P. Characteristics of ca1 neurons recorded intracellularly in the hippocampal in vitro slice preparation. Brain Res 1975;85(3):423–36.
Stuart GJ, Dodt HU, Sakmann B. Patch-clamp recordings from the soma and dendrites of neurons in brain slices using infrared video microscopy. Pflugers Arch 1993;423(5–6):511–8.
Tcheng TK, Gillette MU. A novel carbon fiber bundle microelectrode and modified brain slice chamber for recording long-term multiunit activity from brain slices. J Neurosci Methods 1996;69(2):163–9.
Thiemann W, Malisch R, Reymann K. A new microcirculation chamber for inexpensive long-term investigations of nervous tissue in vitro. Brain Res Bull 1986;17(1):1–4.
Thomson AM, Bannister AP, Hughes DI, Pawelzik H. Differential sensitivity to zolpidem of ipsps activated by morphologically identified ca1 interneurons in slices of rat hippocampus. Eur J Neurosci 2000;12(2):425–36.
Tominaga T, Tominaga Y, Yamada H, Matsumoto G, Ichikawa M. Quantification of optical signals with electrophysiological signals in neural activities of di-4-anepps stained rat hippocampal slices. J Neurosci Methods 2000;102(1):11–23.
White W, Nadler J, Cotman C. A perfusion chamber for the study of cns physiology and pharmacology in vitro. Brain Res 1978;152(3):591–6.
Wu J, Javedan SP, Ellsworth K, Smith K, Fisher RS. Gamma oscillation underlies hyperthermia-induced epileptiform-like spikes in immature rat hippocampal slices. BMC Neuroscience 2001;2:18.
Zbicz KL, Weight FF. Transient voltage and calcium-dependent outward currents in hippocampal ca3 pyramidal neurons. J Neurophysiol 1985;53(4):1038–58.
Zhang CL, Heinemann U. Effects of the triazole derivative loreclezole (r72063) on stimulus induced ionic and field potential responses and on different patterns of epileptiform activity induced by low magnesium in rat entorhinal cortex-hippocampal slices. Naunyn-Schmiedeberg's Arch Pharmacol 1992;346(5):581–7.